15th IFK
Proc. of the 15th International Fluid Power Conference
<DOI>

Experimental study of the influence of the channel geometry of regenerative pumps on their internal flow

VUCEMILOVIC Alexandre[1], RAVELET Florent[2], KOUIDRI Smaïne[3], ESPANET Christophe[4]

1. *MMT (Besançon, France) and LIFSE (ENSAM Paris, France), alexandre.vucemilovic@movingmagnet.com*
2. *LIFSE (ENSAM Paris, France), florent.ravelet@ensam.eu*
3. *LIFSE (ENSAM Paris, France), smaine.kouidri@ensam.eu*
4. *MMT (Besançon, France), Christophe.espanet@movingmagnet.com*

Abstract.

Regenerative pumps are capable of generating high pressures at relatively low flowrates, making them suitable for applications such as electric vehicle cooling systems and cleaning systems for autonomous vehicle sensors. However, their nominal efficiency remains relatively low. The objective of this study is to improve the understanding of how the channel geometry influences the internal flow and performance of regenerative pumps, with particular emphasis on the empirical coefficient of the analytical model. A regenerative pump prototype with variable channel geometry was designed and manufactured. The channel height and width were modified while maintaining a constant side-channel area to enable direct comparison among configurations. The hydrodynamic characteristics, including pressure-flowrate and efficiency-flowrate curves, were experimentally measured. Based on both CFD simulations and experimental data, the empirical coefficients of the analytical model developed by Badami and Mura [1, 2] were estimated, and the corresponding performance predictions were analysed.

Keywords. Regenerative pump, side-channel pump, internal flow, regenerative pump geometry.

1. Introduction

Pumps can be classified into three main categories: centrifugal pumps, axial pumps and volumetric pumps. Centrifugal pumps use the centrifugal force generated by their rotor to project the fluid outward into the volute and toward the outlet. These pumps can produce high flow rates but have small pressure differential between the inlet and outlet (Figure

1.1(a)). Axial pumps have similar characteristics but can generate higher flowrate (Figure 1.1(b)). In contrast, volumetric pumps rely on a variation in volume to draw liquid through the inlet and discharge it through the outlet. They are more efficient at high pressure and large flow rates (Figure 1.1.(c)).

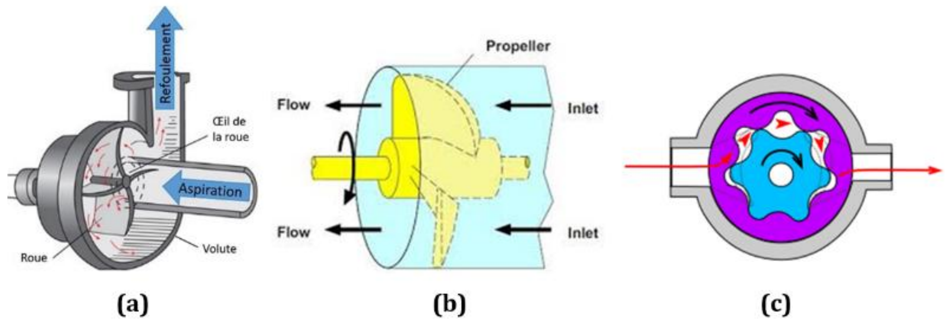

Figure 1.1. Centrifugal pump (a), Axial pump (b) and volumetric pump (gerotor pump) (c)

The pumps described above do not operate efficiently under conditions of low flowrate and high pressure. Regenerative pumps, which combine characteristics of both centrifugal and positive displacement machines, are well adapted to such operating regimes. Applications such as cleaning sensors on autonomous vehicles require compact pumps capable of generating high pressure at low flowrates with good efficiency, conditions for which regenerative pumps are particularly suitable. Introduced in the 1920s by Siemen and Hinsch [3], these pumps are currently used in fluid transfer (oil and gas, boiler feed, cooling and refrigerant systems) and can also be used in mixing and misting applications.

One advantage of this type of pump is its simple design. Its rotor consists of a central bore used for the mounting on a rotating shaft and a series of radially distributed blades around the peripheral surface (Figure 1.2). The symmetry and regular distribution of the blades ensure that the rotor is balanced which minimize vibration and wear. The housing of the pump has a side channel integrated along its inner circumference, aligned with the blades of the rotor (Figure 1.3). It plays a crucial role in the pump operation, that will be explained later. Another key feature of the housing is the stripper, which is a component that separates the inlet and the outlet sections of the pump. This part ensures that the leakages from outlet to inlet are minimal thus improving pump performance.

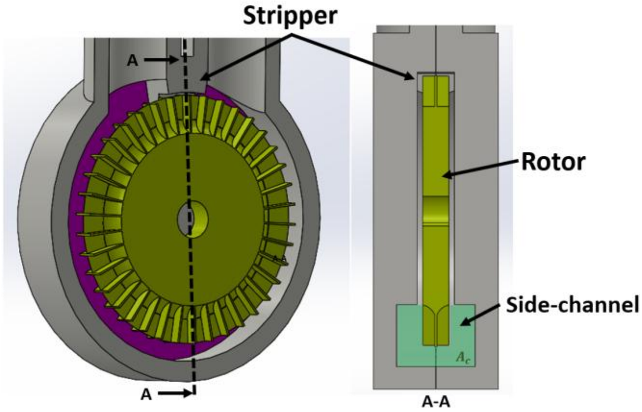

Figure 1.2. Regenerative pump basic design

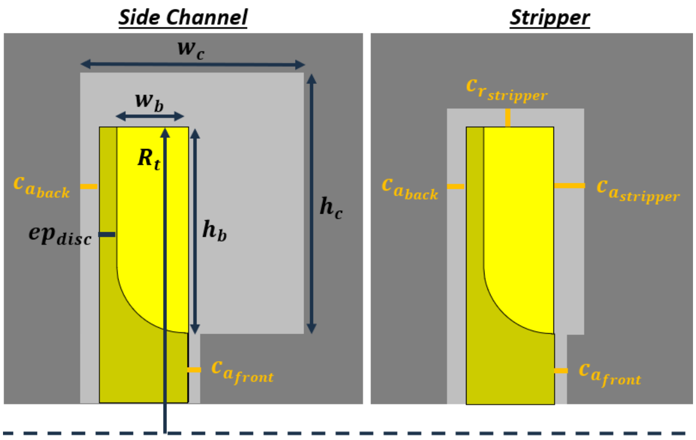

Figure 1.3. Regenerative half-pump geometric parameters

The flow within such a pump is complex and three-dimensional (Figure 1.4). Initially, the fluid enters the pump and is transported by the rotor to the outlet of the housing. Observing from a radial cross-section aligned with a blade, one can also identify a flow referred to as "regenerative" (Figure 1.5). During this flow, the fluid enters at the inner radius of the blade, and the rotation of the wheel increases the fluid's energy. Subsequently, the fluid moves into a channel where various physical phenomena convert a portion of the gained energy into pressure. These phenomena will be explained later. The fluid then returns to the inner radius of the wheel, and the cycle begins anew.

This flow behaviour has been validated by numerous experimental studies and numerical simulations [4-9]. A notable advantage associated with this flow behaviour is the pump's pulsation-free operation. Another advantage is that regenerative pumps are less prone to cavitation compared to centrifugal or volumetric pumps, the gradual increase of the fluid pressure along the pump circumference minimizes turbulent zones that could lead to low-pressure areas. However, regenerative pumps are not immune to cavitation, as shown by

Senoo [4]. This flow behaviour also allows the pumping of liquid/gas mixtures, as gas bubbles are thoroughly mixed with the liquid, breaking down larger gas pockets and evenly distributing the gas within the liquid.

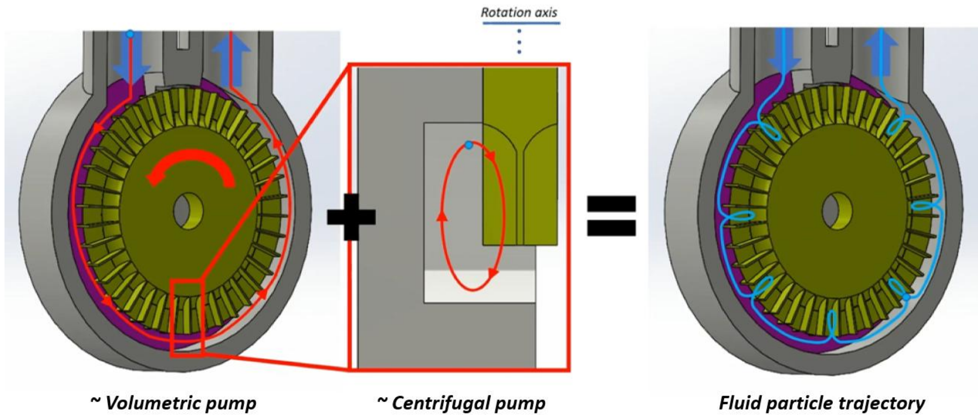

Figure 1.4. Internal flow inside of a regenerative pump

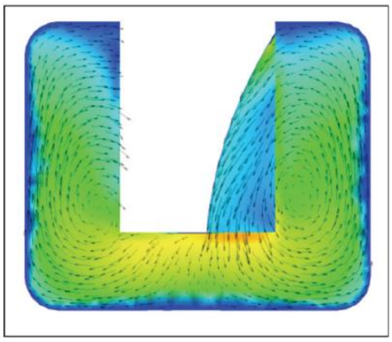

Figure 1.5. Flow inside of the side-channel of a regenerative pump [9]

To predict the characteristic of a regenerative pump, the development of models is essential. Multiple theories have been developed that try to predict the performances of regenerative pumps.

One of these theories is the Momentum Exchange Theory (MET) which was introduced in the 50s by Hopkins and Wilson [5, 6]. In this theory, the mechanism responsible for the pressure generation is the transfer of momentum between the impeller blades and the fluid. The momentum energy imparted to the fluid by the impeller blades propels the fluid to the tip of the blades. Upon entering the pump channel, the fluid's momentum energy is partly converted into pressure through interaction with the turbulence generated by the fixed wall of the outer diameter. Nevertheless, MET is not without limitations. Turbulence mechanism responsible for the pressure rise are simplified and their modelling rely on the use of empirical coefficient. The model then requires experimental data to give accurate results.

The model also relies on several idealized assumptions about flow conditions which can introduce deviations from the actual pump performance.

Since this initial work, several research groups have extended and refined the model [1, 2, 10]. Notably, it has been established that the flowrate in regenerative pumps is strongly influenced by the cross-sectional area of the side channel. Consequently, following definitions for the dimensionless flowrate φ and pressure coefficients ψ of regenerative pumps have been proposed:

$$\varphi = \frac{Q}{UA_c} \quad ; \quad \psi = \frac{2\Delta P}{\rho U^2} \tag{1.1}$$

Here, Q and ΔP are respectively the flowrate and pressure differential between the inlet and the outlet of the pump, A_c the cross-sectional area of the side channel, U the blade tip tangential velocity and ρ the fluid density.

φ and ψ are dimensionless performance coefficients that enable consistent comparison across pumps of varying sizes and rotational speeds. In this study, the definitions given in eq. (1.1) are employed to evaluate and contrast pump configurations featuring different side-channel geometries. By expressing the flowrate and the pressure generated by the pump in nondimensional form, these coefficients isolate the intrinsic dynamic behaviour of each design, allowing performance trends to be interpreted independently of scale or operating conditions.

The paper first introduces the analytical modelling of regenerative pumps. The experimental setup and the tested pump configurations are then described, followed by a presentation of the experimental results. Using both experimental data and CFD simulations, the empirical coefficients of the analytical model are determined and applied to predict pump performance. Finally, a comparison between the predicted and measured efficiency curves is conducted to evaluate the accuracy of the analytical model.

2. REGENERATIVE PUMP MODELLING

The model presented in this section was originally developed by Badami and Mura in 2010 [1] based on Wilson et al. work [6].

To determine the pressure coefficient of the pump, the momentum equation is applied to the fluid in the side-channel:

$$\frac{dK}{dt} = T_p + T_w \tag{2.1}$$

Where K is the angular momentum of the fluid, T_p is the torque associated to the increase in pressure along the pump circumference and T_w is the torque linked to the effect of the shear forces on the side channel walls.

By assuming that the fluid is not compressible and that the torque T_w is proportional to the square of the mean velocity in the channel, equation (2.1) can be rewritten as:

$$Q_m \rho \left(R_t C_{u_2} - r_1 C_{u_1}\right) = A_c r_c \Delta P + \frac{1}{2} K_p A_c r_c \rho u_c^2 \tag{2.2}$$

With R_t the radius of the tip of the impeller, r_c the mean radius of the side channel, r_1 the mean radius of the inlet meridian flow stream at the impeller as defined in Figure 2.1, A_c the cross-section of the side channel, Q_m the recirculation flowrate, C_{u_1} and C_{u_2} the tangential components of the absolute velocity at the entry and exit point of the blades and K_p a coefficient used to model the losses linked to the friction forces on the side channel wall.

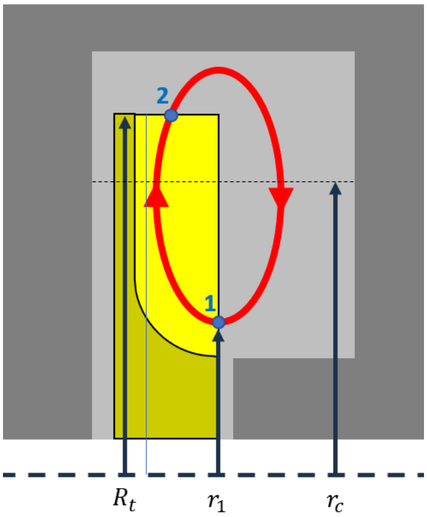

Figure 2.1. Mean flow streamline

the non-dimensional pressure coefficient ψ of the pump can then be determined from equation (2.2):

$$\psi = 2\left(\frac{Q_m}{A_c U}\right)\left(\frac{r_1}{r_c}\right)\left(\frac{R_t}{r_1}\frac{C_{u_2}}{U} - \frac{C_{u_1}}{U}\right) - K_p\varphi^2 \tag{2.3}$$

With φ and ψ the non-dimensional flowrate and pressure coefficients as defined in equation (1.1) and U the tangential velocity of the tip of the blades.

The mean radius of the inlet flow of the impeller can be estimated using the following equation:

$$r_1 = R_t - kh_b \tag{2.4}$$

Where h_b is the height of the blade (Figure 1.3) and k is an unknown coefficient. Badami & Mura use a value of $k \approx \frac{2}{3}$.

Assuming that the angular velocity of the fluid in the side channel is constant along the pump circumference:

$$\frac{C_{u_1}}{U} = \frac{U_{c_1}}{U} = \frac{r_1}{r_c}\varphi \quad ; \quad \frac{C_{u_2}}{U} = \frac{U_2}{U} - \frac{\Delta U_2}{U} = \left(1 - \frac{\Delta U_2}{U_2}\right) \tag{2.5}$$

Here, $\frac{\Delta U_2}{U_2} = \sigma$ is a slip coefficient that considers the velocity difference between the fluid exiting the blades and the fluid in the side channel. Badami & Mura gives the following approximation to estimate its value:

$$\sigma = \frac{2.6}{Z\left(1-\left(\frac{r_1}{R_t}\right)^2\right)+2.6} \tag{2.6}$$

Substituting equation (2.5) in equation (2.3):

$$\psi = 2\left(\frac{Q_m}{A_c U}\right)\left(\frac{R_t}{r_c}(1-\sigma)-\left(\frac{r_1}{r_c}\right)^2 \varphi\right) - K_p \varphi^2 \tag{2.7}$$

In order to estimate the value of the recirculation flowrate Q_m, the energy equation must be applied to the fluid in the vane grooves and in the side channel, with reference to a coordinate system moving with the impeller and the fluid respectively. By summing the obtained equations:

$$K_m\left(\frac{A_c}{A_2}\right)^2\left(\frac{Q_m}{A_c U}\right)^2+\left(\frac{r_1^2-R_t^2}{R_t^2}+\left(\frac{U_{c_2}}{U}\right)^2-\left(\frac{U_{c_1}}{U}\right)^2\right)=0 \tag{2.8}$$

With the assumption that the fluid has a constant angular velocity in the side channel:

$$\frac{Q_m}{A_c U}=\frac{1}{\sqrt{K_m}}\frac{A_2}{A_c}\sqrt{\frac{R_t^2-r_1^2}{R_t^2}-\frac{R_t^2-r_1^2}{r_c^2}\varphi^2} \tag{2.9}$$

Where K_m is a loss coefficient that considers the energy losses due to restrictions and enlargements of the flow in the meridian plane and the losses due to the turbulent shear forces in the vanes, and A_2 is the outlet area of the blades.

This model supposes that there are no internal leakages in the pump. Badami & Mura [1] propose that the real flowrate coefficient φ_R is equal to the difference between the theoretical flowrate coefficient φ and the leakage coefficient φ_f:

$$\varphi_R = \varphi - \varphi_f \tag{2.10}$$

In their pump geometry, there are two main leakages: the leakage through the axial mechanical clearance between the impeller and the housing (φ_{f_1}) and the leakage through the stripper clearances (φ_{f_2}).

Using Bernoulli's equation and assuming the leakage induced by the drag of the impeller through the stripper can be correlated by a triangular drag velocity distribution in the clearance, the leakage flowrate coefficients can be determined:

$$\varphi_{f_1}=\frac{A_{f_1}}{A_c}\frac{1}{\sqrt{K_{f_1}}}\sqrt{\frac{\psi}{2}} \quad ; \quad \varphi_{f_2}=\frac{A_{f_2}}{A_c}\left(\sqrt{\frac{\psi}{Z_s K_{f_2}}}+\frac{1}{2}\frac{r_c}{R_t}\right) \tag{2.11}$$

Where A_{f_1} and A_{f_2} are the leakage areas and Z_s is the number of blades facing the stripper. In those equations, two new loss coefficients appear: K_{f_1} and K_{f_2}. Those coefficients consider the pressure drops in the different leakage areas.

Finally, the efficiency η of the regenerative pump is defined as the ratio between the hydraulic power P_h generated by the pump and the input mechanical power P_m. The hydraulic and mechanical powers can be estimated using the flowrate and pressure coefficient of the pump:

$$P_h = \frac{1}{2}\rho A_c U^3 \varphi_R \psi \tag{2.12}$$

$$P_m = \frac{1}{2} A_c \rho U^3 \frac{r_c}{R_t}\left(\psi + K_p \varphi^2\right) \tag{2.13}$$

$$\eta = \frac{P_h}{P_m} = \frac{R_t}{r_c}\frac{\varphi_R \psi}{\psi + K_p \varphi^2} \tag{2.14}$$

To predict the hydraulic performances of a regenerative pump using this model, the coefficients K_m, K_p, k, K_{f_1} and K_{f_2} must be determined. In [1] those coefficients are considered as constants for a given geometry.

In this study, the effect of the leakages will be neglected ($K_{f_1} = K_{f_2} = 0$) and K_p and k will be determined using CFD simulations. The value of K_m will then be estimated from experimental data.

3. EXPERIMENTAL SETUP AND RESULTS

The previously described model will be applied to the following pump prototype (Figure 3.1).

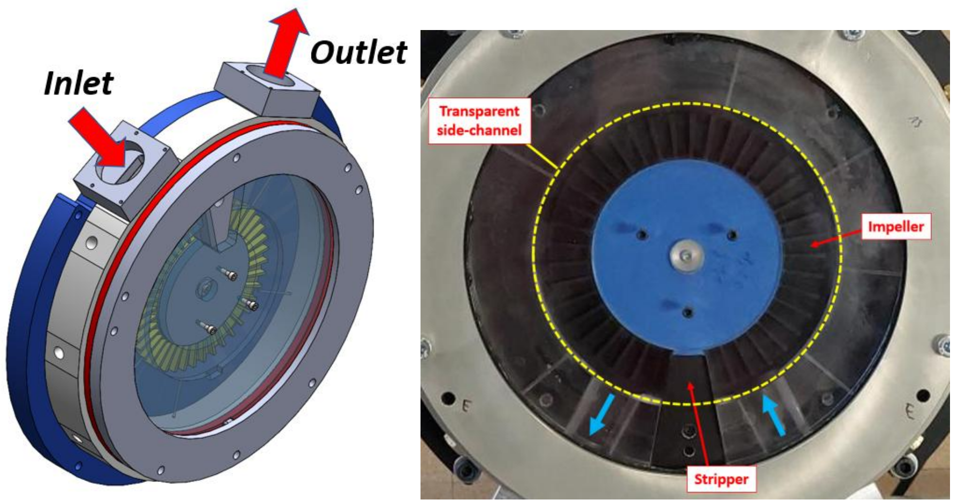

Figure 3.1. Regenerative pump prototype

This prototype is a half regenerative pump (Figure 1.3). Unlike a full regenerative pump, in which the regenerative flow is on both side of the impeller, the half regenerative pump only features one regenerative flow in the side channel. This design simplifies the manufacturing and allows for focused investigation of regenerative flow behaviour while retaining the core operating principles of regenerative pumps. Theoretically, a half regenerative pump can achieve the same pressure head as a full regenerative pump, but its flowrate is reduced by half due to the single-sided channel. However, this design introduces an axial clearance c_{a1} between the impeller and the housing (Figure 1.3), in which the fluid can flow. This creates internal leakages and viscous frictions that do not exist in the full pump configuration, impacting the performances of the pump.

Table 3.1. Constant geometrical parameters

$\boldsymbol{R_t}$	$\mathbf{82.5\ mm}$	$\boldsymbol{c_{a_{back}}}$	$\mathbf{0.7\ mm}$
$\boldsymbol{w_b}$	$8.5\ mm$	$c_{a_{front}}$	$0.25\ mm$
$\boldsymbol{h_b}$	$26.25\ mm$	$c_{a_{stripper}}$	$0.5\ mm$
$\boldsymbol{ep_{disc}}$	$2\ mm$	$c_{r_{stripper}}$	$0.5\ mm$

Despite the constraints of the design, the channel geometry can be easily modified, and multiple pump configurations have been manufactured (Table 3.1 and Figure 3.2).

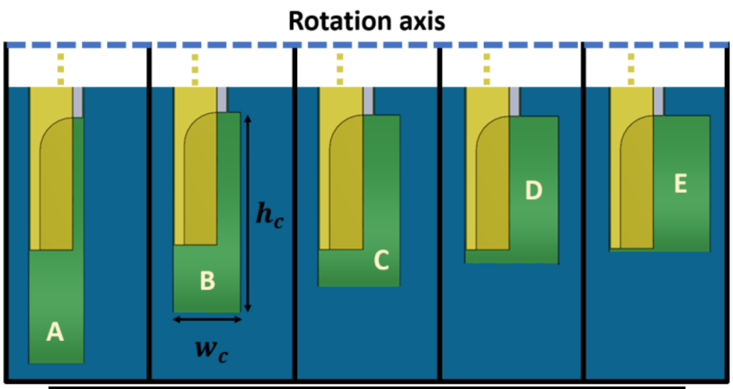

Configuration	w_c	h_c
A	$11\ mm$	$48.75\ mm$
B	$13.5\ mm$	$39.7\ mm$
C	$16\ mm$	$33.5\ mm$
D	$18.5\ mm$	$29\ mm$
E	$20\ mm$	$26.8\ mm$

Figure 3.2. Geometric configurations of the channel

To evaluate the performance of this half regenerative pump prototype, a dedicated hydraulic test bench was developed. This setup allows for the measurement of key hydraulic and mechanical parameters.

The test bench consists of a closed-loop circuit equipped with a variable speed electric motor driving the pump. A torquemeter equipped with an incremental encoder allows for the measurement of the input torque T_{exp} and rotational speed ω_{exp} of the impeller leading to the computation of the input mechanical power. The flowrate Q_{exp} is measured using an ultrasonic flowmeter installed downstream of the pump, while pressure sensors mounted upstream and downstream of the pump provide measurements of the pressure differential of the pump $\Delta P_{exp} = P_{outlet} - P_{inlet}$. A data acquisition system records all sensor outputs for post-processing and performance evaluation of the different pump configurations. The circuit also includes a fluid tank to minimize air entrainment as well as a regulation valve used to modify the flow' resistance and simulate different operating conditions (Figure 3.3). A temperature sensor and a barometer mounted on the fluid tank allows for the control of the fluid temperature and of the hydrostatic pressure inside of the hydraulic circuit. Pressure sensors mounted on the circumference of the pump also allows for the measurement of the pressure gradient inside of the pump but this experimental data will not be investigated in this paper.

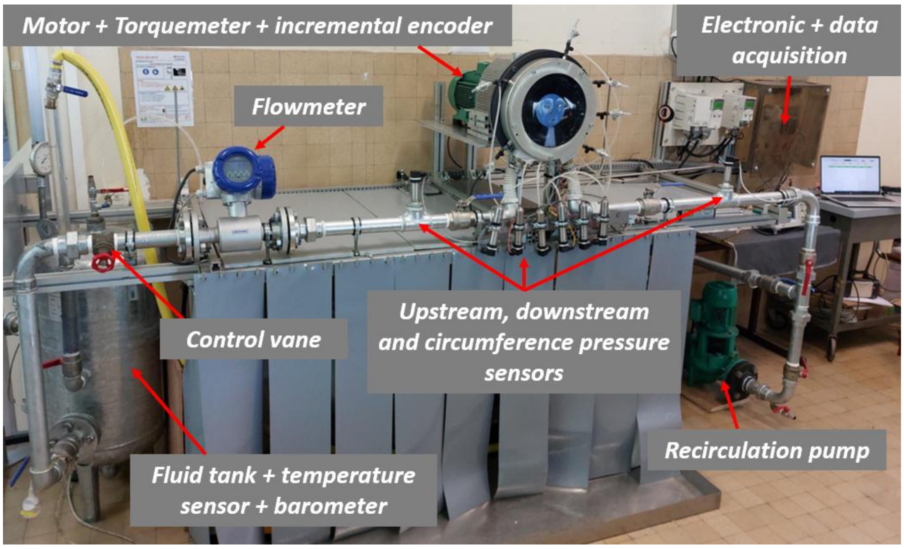

Figure 3.3. Hydraulic test bench

For each configuration, the pump rotational speed was maintained at a constant value, and the pressure drop of the hydraulic circuit was progressively increased by adjusting the control valve, enabling measurement of the pump flow/pressure and flow/efficiency characteristics.

Experimental results at 900 RPM (configurations A to D) are presented in Figure 3.4. Due to manufacturing issues encountered with configuration E, its performance could not be measured at 900 RPM; therefore, the results obtained at 600 RPM are reported instead.

φ_{exp} and ψ_{exp} have been calculated from experimental flowrate, pressure differential and rotational speed data using the formulas presented in eq.(1.1). The experimental efficiency was calculated from flowrate, pressure, torque and rotational speed measurements:

$$\eta_{exp} = \frac{Q_{exp}\Delta P_{exp}}{T_{exp}\omega_{exp}} \tag{3.1}$$

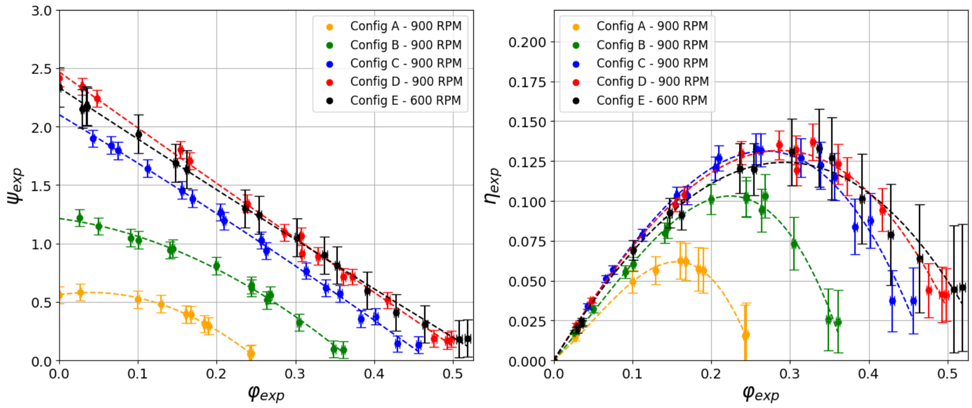

Figure 3.4. Experimental results

The study of the coefficient K_m will be conducted on configuration C at 900 RPM (blue curves on Figure 3.4).

4. Estimation of K_m

As mentioned in Chapter 2, leakage effects are neglected in this study. Using equations (2.3) and (2.9), an expression for the recirculation loss coefficient K_m can be derived:

$$K_m = \frac{4A_2^2(R_t^2 r_c^2 - R_t^2\varphi^2(R_t^2 - r_1^2) - r_1^2 r_c^2)(R_t r_c(\sigma - 1) - r_1^2\varphi)^2}{A_c^2 R_t^2 r_c^6\left(\psi + K_p\varphi^2\right)^2} \tag{4.1}$$

In this formulation, K_m is expressed in terms of known geometric parameters (R_t, r_c, A_2), dimensionless flowrate and pressure coefficient (φ, ψ) and unknown parameters σ, r_1 and K_p. The slip coefficient σ can be evaluated from eq. (2.6). The remaining two coefficients, K_p and k are determined via CFD simulations.

K_p represents the pressure drops in the pump's inlet, outlet and side channel. A simplified CFD simulation of these regions, excluding the impeller, enables the evaluation of the pressure drop generated by the pump. Experimental measurements were also performed using an impeller without blades and the recirculation pump installed on the test bench to produce the required flowrates (Figure 4.1).

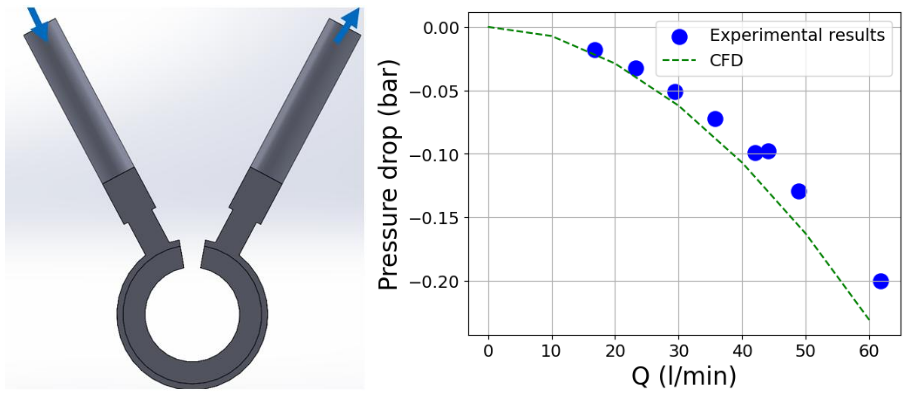

Figure 4.1. CFD geometry and comparison of experimental and CFD results

The experimental data and CFD predictions are in close agreement, with a minor deviation of approximately 25 mbar at high flowrates, attributable to leakage paths not included in the simulation. This agreement enables an accurate estimation of the pressure drop in complex channel geometries.

From the pressure drop curve estimated by CFD simulation, the value of K_p can then be determined:

$$K_p = \frac{2\Delta P_l}{\rho v^2} = \frac{2\Delta P_l}{\rho (Q/A_c)^2} \tag{4.2}$$

Where ΔP_l is the pressure drop at the flowrate Q and $v = \frac{Q}{A_c}$ is the fluid velocity in the side-channel. For configuration C, $K_p = 4.5$. Badami & Mura [2] reported a value of $K_p = 3.5$ for a regenerative air compressor with similar geometry, deriving the coefficient through conventional pressure-drop analysis.

The coefficient k is then evaluated from the velocity field in the side channel within a meridional plane. The radius r_1 is assumed to correspond to the center of the impeller inlet height. For configuration C, $k \approx 0.66$ (Figure 4.2) corresponding to the value used by Badami & Mura [2].

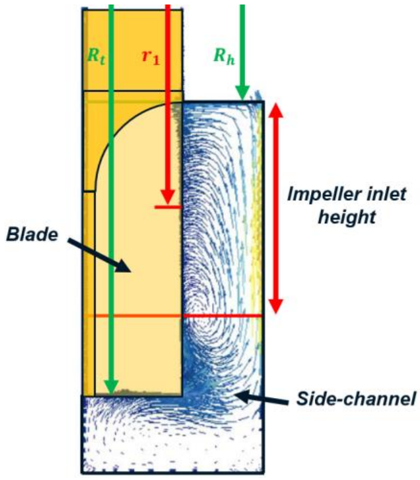

Figure 4.2. Flow in the meridional plane in configuration C at 900 RPM

With the values of K_p and k determined, K_m can be calculated from eq.(4.1) using the experimental φ and ψ data (Figure 4.3). In Badami's model [1], K_m is a constant loss coefficient. The mean value of the obtained K_m curve is then used. For configuration C, $K_m \approx 24.9$.

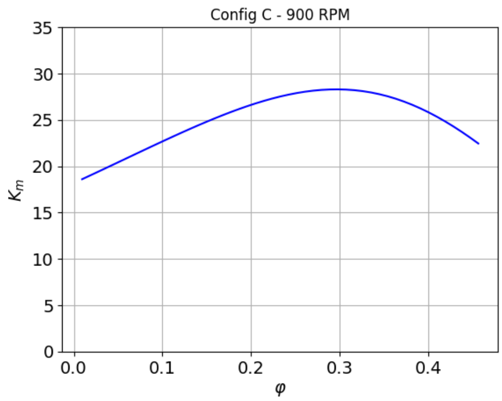

Figure 4.3. Calculated K_m for configuration C at 900 RPM

The obtained values of K_p, k and K_m enable prediction of pump performance through eqs. (2.3) and (2.14) (Figure 4.4).

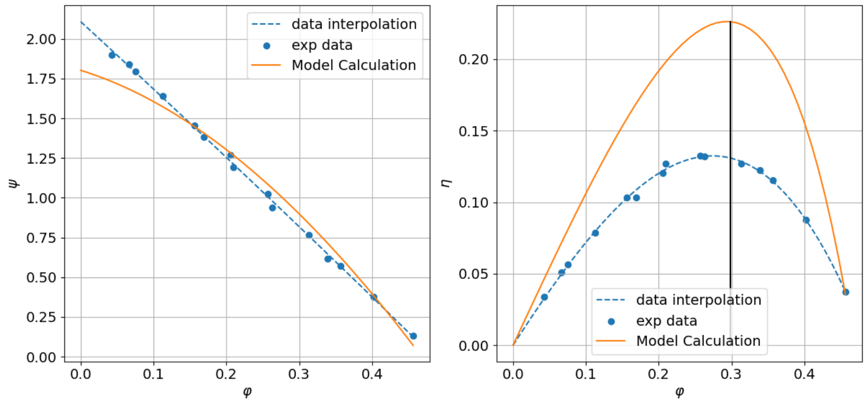

Figure 4.4. Computed pump performance and comparison to experimental data

Overall, the analytically derived $\psi = f(\varphi)$ curve (Figure 4.4) fit closely with experimental data. The predicted efficiency of the pump is overestimated because of neglected losses. However, the optimal flowrate of the pump is accurately captured.

Applying the same methodology to the remaining pump configurations demonstrates how channel geometry influences overall pump performance.

5. CHANNEL GEOMETRY INFLUENCE

In equation (2.3), the influence of the channel geometry is reflected in r_c, the mean channel radius of the pump, and in the loss coefficient K_p. Both parameters exhibit similar trends, decreasing from configuration A to configuration E (Figure 5.1).

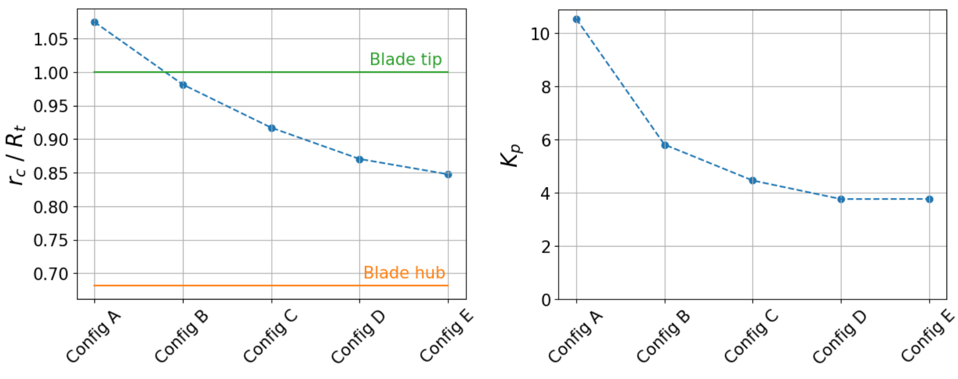

Figure 5.1. r_c and K_p values for each configuration

Variations in the channel geometry also affect the pump's efficiency curve. Figure 5.2 illustrates that configurations with smaller r_c exhibit higher maximum efficiency and a larger optimum flowrate, with an asymptotic trend observed around configuration D. The tendencies are consistent with both experimental and analytical results. A slight decrease in η_{max} is observed for configuration E, which can be attributed to the difference in pressure resulting from the lower rotational speed, leading to a larger measurement error in the pressure sensors. This asymptotic behaviour around configuration D can also be seen in the variations of K_m (Figure 5.3).

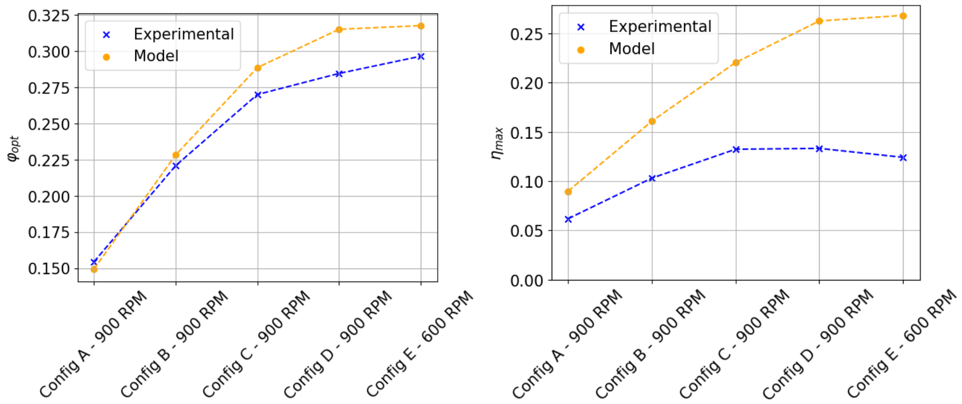

Figure 5.2. η_{max} and associated flowrate coefficient for each configuration

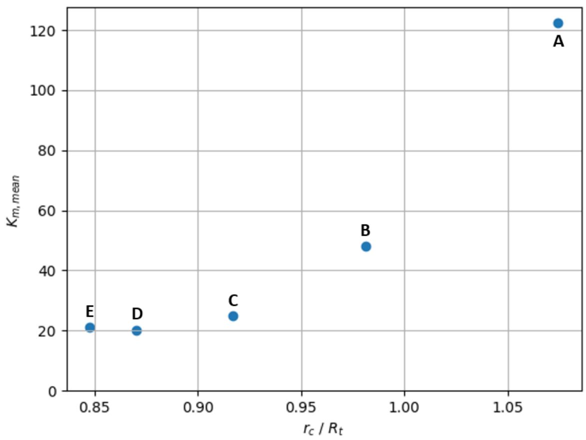

Figure 5.3. Mean K_m calculated for each configuration

6. CONCLUSION

This study provided further insight into the influence of side-channel geometry on the performance of regenerative pumps, with particular focus on the empirical coefficients of the model developed by Badami and Mura [1], based on the earlier work of Wilson et al. [6]. The loss coefficient K_p and the geometric coefficient k were estimated using CFD simulations, enabling the subsequent computation of the recirculation loss coefficient K_m. The model's efficiency predictions did not accurately reproduce the absolute efficiency values due to neglected losses, but they provided a good estimation of the optimum flowrate coefficient when compared with experimental data.

In the present study, leakage effects were neglected and the coefficient k was assumed constant. Future work will address the role of mechanical clearances in the pump, aiming to refine the characterisation of their impact on internal flow dynamics and overall performance, while also examining the variability of k through CFD simulations.

7. REFERENCES

[1] M. Badami and M. Mura, “Theoretical model with experimental validation of a regenerative blower for hydrogen recirculation in a PEM fuel cell system,” *Energy Conversion and Management,* vol. 51, pp. 553-560, 2010.

[2] M. Badami and M. Mura, “Setup and validation of a regenerative compressor model applied to different devices,” *Energy Conversion and Management,* vol. 52, pp. 2157-2164, 2011.

[3] O. Siemen and J. Hinsch, “Teilweise beafschlagte umlaufpumpe mit dichtender, kreisender hilfsflüssigkeit”. Patent DE413435C, 1920.

[4] Y. Senoo, “Theoretical research on friction pump,” *Reports of the Research Institute for Fluid Engineering, Kyushu University,* vol. 5, pp. 23-38, 1948.

[5] T. J. Hopkins and L. R. Lazo, “Theoretical and experimental analysis of a regenerative turbine pump,” *Bachelor of Science thesis, Massachusetts Institute of Technology,* 1953.

[6] W. A. Wilson, M. A. Santalo and J. A. Oelrich, “A Theory of the Fluid-Dynamic Mechanism of Regenerative Pumps,” *Journal of fluid engineering,* vol. 77, no. 8, pp. 1303-1311, 1955.

[7] D. Dewitt, “Rational design and development of the regenerative pump,” *PhD thesis, Massachusetts Institute of Technology,* 1957.

[8] F. Quail, T. Scanlon and M. Stickland, “Study of a regenerative pump using numerical and experimental techniques,” *8th European Turbomachinery Conference,* 2009.

[9] J. Nejadrajabali, A. Riasi and S. A. Nourbakhsh, “Flow Pattern Analysis and Performance Improvement of Regenerative Flow Pump Using Blade Geometry Modification,” *International Journal of Rotating Machinery,* vol. 2016, pp. 1-16, 2016.

[10] F. Quail, F. Scanlon and A. Baumgartner, “Design study of a regenerative pump using one-dimensional and three-dimensional numerical techniques,” *European Journal of Mechanics - B/Fluids,* vol. 31, pp. 181-187, 2012.

Biographies

Alexandre Vucemilovic received the engineering diploma in Mechatronics and Robotics from ENSMM (Besançon, France) and the master's degree in Microsystems, Instrumentation and Robotics from the University of Bourgogne-Franche-Comté in 2022. He is currently working as a R&D engineer at moving Magnet Technologies (Besançon, France) and pursuing a Ph.D. at LIFSE, ENSAM (Paris, France), focusing on improving the understanding and modelling of regenerative pumps.

Florent Ravelet received the master's degree in marine engineering from ENSTA in 2002, and the philosophy of doctorate degree in Fluid Mechanics from Polytechnique in 2005, respectively. He is currently working as a Full Professor at the Laboratory LIFSE, Arts et Metiers Science and Technology. His research areas include turbulent flows, cavitation and turbomachinery.

Smaïne Kouidri is a Professor at Arts et Métiers Institute of Technology (ENSAM). He graduated in 1990 from Arts & Métiers ParisTech where he received his Ph.D. in 1993. He then became an associate professor at ENSAM until 2007, when he joined the Computer Sciences Laboratory for Mechanics and Engineering Sciences (LIMSI), a CNRS laboratory UPR 3251. He later became the director of the ENSAM Paris Campus (2021-2023) before joining the Laboratory of Fluid Engineering and Energy Systems (LIFSE). His research activities fall within the general area of internal flows in turbomachinery, aeroacoustics and thermoacoustics and his main research focus is the development and the implementation of models for reducing noise pollution and improving the efficiency of conversion energy systems such as Pumps, compressors and fans.

Christophe Espanet received his Ph.D. degree in Electrical Engineering from the University of Franche-Comté, France, in 1999. His doctoral research focused on the optimal design of permanent magnet brushless DC in-wheel motors. From 1999 to 2015, he served as Assistant Professor and later Full Professor at the University of Franche-Comté. He is currently the Scientific Director of the Sonceboz Group, where he leads research teams at Moving Magnet Technologies, developing innovative mechatronic solutions.